

Observations of interfaces in direct wafer-bonded InP–GaAs structures

Yan-feng Lao, Hui-zhen Wu, and Ming Li

Citation: *J. Vac. Sci. Technol. B* **23**, 2351 (2005); doi: 10.1116/1.2102968

View online: <http://dx.doi.org/10.1116/1.2102968>

View Table of Contents: <http://avspublications.org/resource/1/JVTBD9/v23/i6>

Published by the AVS: Science & Technology of Materials, Interfaces, and Processing

Related Articles

Si delta doping inside InAs/GaAs quantum dots with different doping densities

J. Vac. Sci. Technol. B **30**, 041808 (2012)

Factors controlling the resistance of Ohmic contacts to n-InGaAs

J. Vac. Sci. Technol. B **30**, 031209 (2012)

Blueshift in sulfur treated GaAsP/AlGaAs near surface quantum well

J. Vac. Sci. Technol. A **30**, 021401 (2012)

Structural and luminescent properties of bulk InAsSb

J. Vac. Sci. Technol. B **30**, 02B105 (2012)

Suppressed phase separation in thick GaInAsSb layers across the compositional range grown by molecular beam epitaxy for 1.7–4.9 μm infrared materials

J. Vac. Sci. Technol. B **30**, 02B104 (2012)

Additional information on *J. Vac. Sci. Technol. B*

Journal Homepage: <http://avspublications.org/jvstb>

Journal Information: http://avspublications.org/jvstb/about/about_the_journal

Top downloads: http://avspublications.org/jvstb/top_20_most_downloaded

Information for Authors: http://avspublications.org/jvstb/authors/information_for_contributors

ADVERTISEMENT

AVS 59th International Symposium & Exhibition
October 28–November 2, 2012 • Tampa, Florida

 212-248-0200
avsnyc@avs.org
www.avs.org



DIVISION/GROUP PROGRAMS:

- Advanced Surface Engineering
- Applied Surface Science
- Biomaterial Interfaces
- Electronic Materials & Processing
- Magnetic Interfaces & Nanostructures
- Manufacturing Science & Technology
- MEMS & NEMS
- Nanometer-Scale Science & Technology
- Plasma Science & Technology
- Surface Science
- Thin Film
- Vacuum Technology

FOCUS TOPICS:

- Actinides & Rare Earths
- Biofilms & Biofouling: Marine, Medical, Energy
- Biointerphases
- Electron Transport at the Nanoscale
- Energy Frontiers
- Exhibitor Technology Spotlight
- Graphene & Related Materials
- Helium Ion Microscopy
- *InSitu* Microscopy & Spectroscopy
- Nanomanufacturing
- Oxide Heterostructures-Interface Form & Function
- Scanning Probe Microscopy
- Spectroscopic Ellipsometry
- Transparent Conductors & Printable Electronics
- Tribology

Observations of interfaces in direct wafer-bonded InP–GaAs structures

Yan-feng Lao and Hui-zhen Wu^{a)}

State Key Laboratory of Functional Materials for Informatics, Shanghai Institute of Microsystem and Information Technology, Chinese Academy of Sciences, 865 Changning Road, Shanghai 200050, China

Ming Li

Analytical Laboratory, Reliability Engineering, Semiconductor Manufacturing International (Shanghai) Corporation, 18 Zhangjiang Road, PuDong New Area, Shanghai 201203, China

(Received 14 December 2004; accepted 6 September 2005; published 31 October 2005)

Direct wafer-bonded InP–GaAs structures were studied by cross-sectional observations using a field-emission scanning-electron microscope (FESEM) and by infrared-absorbance spectra using a Fourier-transform infrared spectroscopy. FESEM observations demonstrate that the interfaces of 560 and 580 °C bonded InP–GaAs structures are smooth and uninterrupted, while interfacial gaps appear for the samples bonded at 620 and 680 °C. However, large dimensional areas of bonding interfaces cannot be observed by FESEM because its inspection size is limited to microregions. Experimental results show that infrared-absorbance measurements can be an effective method for quality examination of bonded InP–GaAs structures. By soaking wax into poorly bonded interfaces and using its absorption characteristics at 3.383, 3.426, and 3.509 μm , interfacial gaps are indirectly measured by infrared spectra. Absorbance-intensity mappings at absorption peaks were used to image poorly bonded areas. Thus the interface quality of the whole wafer-bonded sample can be seen clearly. Nonuniform pressure applied over the sample during annealing step accounts for poorly bonded interfaces. Using the improved fixture, uniformly bonded InP–GaAs structures that do not have interfacial gaps were obtained. © 2005 American Vacuum Society.
[DOI: 10.1116/1.2102968]

I. INTRODUCTION

High-quality III-V materials have been successfully grown by molecular-beam epitaxy and metalorganic chemical-vapor deposition, which improves the performance of device structures. The device performance, however, is eventually limited by the intrinsic material properties. Different materials have their unique optical and electrical properties. Thus, structures consisting of two different materials are expected to exhibit high device performance. But these structures are generally hard to fabricate by epitaxial growth methods due to lattice mismatch. In recent years direct wafer-bonding (or wafer-fusion) technologies used in Si-based structures^{1,2} have been successfully developed for III-V compound semiconductor assembly.^{3–6} Edge-emitting lasers,⁷ vertical-cavity surface-emitting laser structures,⁸ detector structures,⁹ vertical coupler structures,¹⁰ and monolithic-material integration by nonplanar wafer bonding,¹¹ have been successfully fabricated by this technique and show superior device performance. Although a scale of 1 cm \times 1 cm wafer bonding is enough for experimental studies, industrial applications require large-scale wafer bonding. However, the uniformity of the bonding interface is still a problem. Recently, whole InP and GaAs substrates have been uniformly bonded without mechanical pressure by the atomic-hydrogen surface cleaning and low-temperature bonding method,¹² which is expected to be an

alternative method for industrial applications. But this method requires very clean surfaces for bonding and should be carried out under an ultrahigh vacuum (UHV) ($<5 \times 10^{-11}$ Torr) background. The bonding of InP–GaAs epitaxial layers and electrical characteristics of bonded structures has not yet been demonstrated. Detecting and improving the quality and uniformity of high-temperature bonded large-scale structures remain important.

Transmission-electron microscope (TEM) observations^{5,13} and electrical characteristics^{6,14} of wafer-bonded InP–GaAs structures have been extensively studied. However, these methods are inconvenient for checking the quality of the bonded interface. TEM can only check microregions. Although electrical characterizations can show the interface quality to a certain degree, the preparation of samples is inconvenient. Furthermore, the bonding temperature, pressure, and annealing time all have an effect on electrical properties of bonded structures. The quality criterion of electrical measurement is indefinite. Other methods such as electron-beam induced-current (EBIC) maps¹⁵ and cathodoluminescence (CL)¹⁶ images have been used in defect detection for relatively large dimensional bonded structures. These methods give direct views of interfaces. But they require the fabrication of special structures. For instance, contact electrodes of bonded structures are required for EBIC measurement and bonded samples need InGaAsP layers as luminescence-exciting mediums in CL imaging.

For this article, we directly bonded InP–GaAs structures at different temperatures. Their interfaces were checked by

^{a)}Author to whom correspondence should be addressed; electronic mail: hzwu@mail.sim.ac.cn

field-emission scanning-electron microscope (FESEM). To effectively detect poorly bonded areas (containing interfacial cavities), InP–GaAs structures were processed with molten wax. By soaking wax into poorly bonded interfaces, the absorption intensity at 3.383, 3.426, and 3.509 μm of transitions characteristic of the wax reflect the interface bonding quality. It was found that the proportion of poorly bonded areas in the samples bonded at higher temperatures was greater than those bonded at lower temperatures, which is attributed to the nonuniform pressure applied to wafers during the bonding processes. By improving the fixture, uniformly bonded InP–GaAs structures with the absence of interfacial gaps were obtained.

II. EXPERIMENT

The wafers used for bonding were commercial InP and GaAs substrates. They were cleaved into about 1 cm \times 1 cm squares along the $\langle 110 \rangle$ direction. First, the substrates were cleaned by isopropanol, acetone, and ethanol sequentially in an ultrasonic bath, then rinsed by deionized (DI) water, and finally dried with N_2 . The InP wafers were etched in aqueous-based $\text{H}_2\text{SO}_4 + \text{H}_2\text{O}_2 + \text{H}_2\text{O}$ (3:1:1) solutions and the GaAs wafers were etched in aqueous-based $\text{H}_2\text{SO}_4 + \text{H}_2\text{O}$ (1:20) solutions for surface oxide removal. After rinsing in DI water, InP and GaAs wafers were all dipped into aqueous-based hydrogen fluoride solutions ($\text{HF} + \text{H}_2\text{O} = 1:10$) for surface passivation. In our experiment, the surface of the InP substrate was hydrophilic and the GaAs substrate was hydrophobic after being etched by aqueous-based $\text{HF} + \text{H}_2\text{O}$ (1:10) solutions. Finally, they were joined and put face-to-face with the $\langle 110 \rangle$ direction aligned into a steel fixture. This fixture was placed into a furnace for annealing in a flowing N_2 ambient. The bonding pressure and annealing time were fixed to ~ 5 MPa and 35 min, respectively, while different bonding temperatures (560, 580, 620, and 680 $^\circ\text{C}$) were used. After bonding, the InP–GaAs structures were thinned to ~ 120 μm for the InP side and ~ 150 μm for the GaAs side.

In our experiments, it was interesting that when single InP (or GaAs) substrates were covered with a thin wax the infrared absorption spectra showed three strong absorption peaks at 3.383, 3.426, and 3.509 μm , while without wax coverage the substrates were transparent at these characteristic lines. We utilized these characteristic absorption lines of wax to characterize the bonded InP–GaAs interfaces. The bonded InP–GaAs samples were processed with wax by the following steps described here. First, the bonded samples were heated to 100 $^\circ\text{C}$ and immersed into molten wax for one minute. Then they were cleaned using organic solutions (carbon tetrachloride, acetone, and ethanol in sequence). Thus the surfaces of the bonded InP–GaAs structures were clean and free of wax, but the wax penetrated into the interfacial cavities. The infrared-absorbance spectra were measured by a NICOLET 860 Fourier-transform infrared (FTIR) spectroscopy. Thinned InP (~ 150 μm) and GaAs (~ 150 μm) substrates were used as reference samples for background signal removal. The cross sections of wafer-bonded InP–GaAs

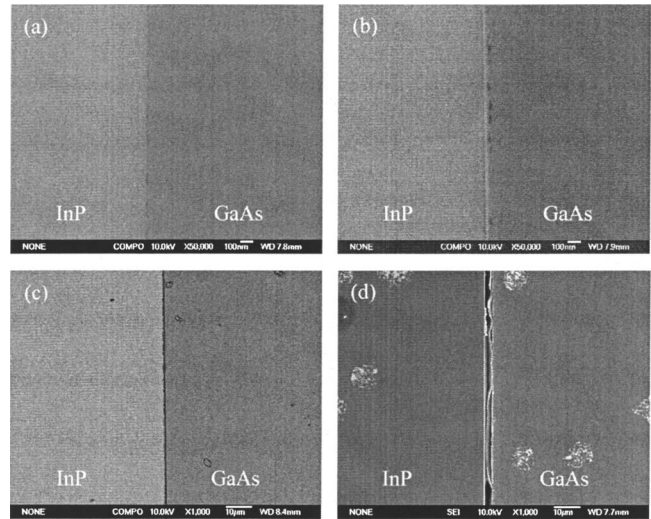


FIG. 1. FESEM cross sections of the InP–GaAs structures bonded at (a) 560 $^\circ\text{C}$, (b) 580 $^\circ\text{C}$, (c) 620 $^\circ\text{C}$, and (d) 680 $^\circ\text{C}$.

structures were observed using a JEOL JSM-6700F field-emission scanning-electron microscope (FESEM).

III. RESULTS AND DISCUSSION

A. FESEM cross-sectional observations of InP–GaAs bonded structures

Figures 1(a), 1(b), 1(c), and 1(d) are micrographs of FESEM cross sections for structures bonded at 560, 580, 620, and 680 $^\circ\text{C}$, respectively, in which the cleavage facets for cross-sectional observations were acquired unintentionally. The InP–GaAs interfaces of the 560 and 580 $^\circ\text{C}$ bonded samples as shown in Figs. 1(a) and 1(b) are smooth and appear to be one material except for some randomly distributed black spots. These black spots may be interfacial cavities resulting from voids' aggregation,¹⁷ indium depletion,¹³ or dislocation networks¹⁵ which relax and accommodate lattice mismatch, thermal strain, twist misorientation, and tilt misfit between the two materials. The bright line on the micrograph of Fig. 1(b) results from a height difference of two bonded wafers following cleavage. However, poorly bonded interfaces were observed in samples annealed at 620 and 680 $^\circ\text{C}$. Figures 1(c) and 1(d) show a gap at the interface of two wafers. This interfacial gap is partly filled with materials disassociated from two wafers. It seems that the quality of the bonded InP–GaAs structures annealed at higher temperatures is worse than that of wafers annealed at lower temperatures, which is a paradox in comparison with previous reports.^{5,13,17} Poorly bonded areas could be attributed to nonuniform pressure applied to the InP–GaAs wafers during the annealing stage. In local low-pressure areas, the joint of the InP and GaAs surface was not close so that interfacial elements were decomposed and lost upon the annealing process. With increasing annealing temperatures, the decomposition and loss of interfacial materials was possibly enhanced. Thus in this area dense interfacial cavities were formed under higher annealing temperatures. The nonuniform pressure ef-

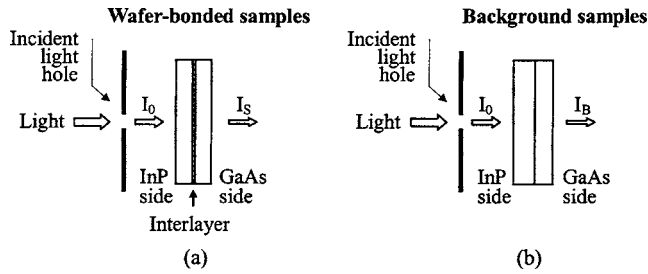


FIG. 2. Schematic diagram of FTIR measurement of (a) the InP–GaAs bonded structures, in which an interlayer at interface is assumed, and (b) the InP+GaAs background samples.

fects and its improvement will be discussed in Sec. III C. With the infrared-absorbance evaluation, cavities that result from the nonuniform bonding pressure can be imaged.

B. Infrared-absorbance evaluation of interfaces of InP–GaAs bonded structures

The schematic diagram of the arrangement for the infrared-absorbance spectra measurements is shown in Fig. 2. Assuming that d_A , d_I , d_B and α_A , α_I , α_B are the thicknesses and absorption coefficients of InP, interlayer, and GaAs, respectively, for bonding structures, and d_{A0} , d_{B0} are the thicknesses of the InP substrate and GaAs substrate for background measurements, then

$$I_S = I_0 e^{-\alpha_I d_I - (\alpha_A d_A + \alpha_B d_B)}, \quad (1)$$

$$I_B = I_0 e^{-(\alpha_A d_{A0} + \alpha_B d_{B0})}. \quad (2)$$

Thus

$$I_S = I_B e^{-[\alpha_A(d_A - d_{A0}) + \alpha_B(d_B - d_{B0})]}. e^{-\alpha_I d_I}. \quad (3)$$

The absorbance is defined as follows:

$$A = -\log_{10}(I_S/I_B) = C + \log_{10}^e \cdot \alpha_I d_I, \quad (4)$$

where

$$C = [\alpha_A(d_A - d_{A0}) + \alpha_B(d_B - d_{B0})] \log_{10}^e. \quad (5)$$

In our experiment, the infrared spectra were measured in the wavelength range from 1.0 to 4.0 μm . Thus InP and GaAs substrates do not have strong light absorption bands in this region because the band gaps at room temperature for these two materials are 1.34 and 1.42 eV. Figure 3 shows the absorbance spectra of the InP+GaAs substrate and wax. The intensity fluctuation between 2.6 and 2.8 μm is due to the absorption of carbon dioxide and water vapor in the atmosphere because the FTIR measurements were carried out in atmospheric ambient.

The typical absorbance spectra of the wax-processed InP–GaAs bonded samples are shown in Figs. 4(a) and 4(b), respectively. We can see that absorption peaks at 3.383, 3.426, and 3.509 μm appear in both spectra of 560 and 680 $^\circ\text{C}$ bonded samples. These peaks tell us that a certain material appears at the InP–GaAs interface indicating the poorly bonded area. In addition, spectra with the absence of these absorption peaks were observed as well. Thus, the InP–GaAs

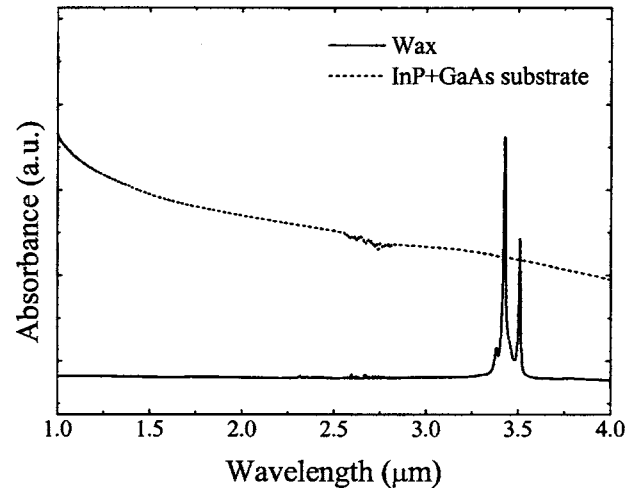


FIG. 3. Absorbance spectra of the InP+GaAs substrate and wax.

structures were nonuniformly bonded. We ascribe this result to the nonuniform pressure during annealing step which will be explained later.

As it is known that the band gap absorption wavelength of the binary compound InAs at room temperature is at about 3.5 μm as well. To exclude the absorption at 3.5 μm being due to InAs material at the interface, a low-temperature absorbance spectrum for the 560 $^\circ\text{C}$ bonded samples was measured. When the temperature is lowered to 250 K, the band gap wavelength of InAs should have a blueshift. However, no blueshift of absorption peaks was observed in the spectrum taken at 250 K, as shown in Fig. 4(c). So the product generated by III-V elements of the interfacial InP and GaAs during annealing step does not obviously contribute to the absorption characteristic of the interface in Figs. 4(a) and 4(b). Further, we compared absorption spectra measured before and after soaking wax to the poorly bonded samples. It was found that after wax soakage of the poorly bonded samples strong absorption peaks at 3.383, 3.426, and 3.509 μm were present, while prior to wax soakage no absorption peaks were observed. Further studies showed the intensity of the absorption is proportional to the wax content in the interface. Therefore the wax in the interface can be used as an infrared-absorbance detecting medium.

Because the thicknesses of InP and GaAs substrates of wafer-bonded and background samples are nearly equal, from Eqs. (4) and (5) it can be seen the constant C can be ignored. Thus the absorbance intensity at peaks (3.383, 3.426, and 3.509 μm) defines the dimension of interfacial cavities, i.e., the interface quality of wafer bonding which will be shown in the next section.

By measuring absorbance spectra at different areas (positions), we can check the bonding uniformity of the interface. Figures 4(a) and 4(b) show the six-area spectra of InP–GaAs structures bonded at 560 and 680 $^\circ\text{C}$, respectively. It can be seen that the poorly bonded areas for the higher-temperature annealed sample are larger than those for the lower-temperature annealed sample.¹⁸ This result is consistent with the FESEM cross-sectional observation of the poorly bonded

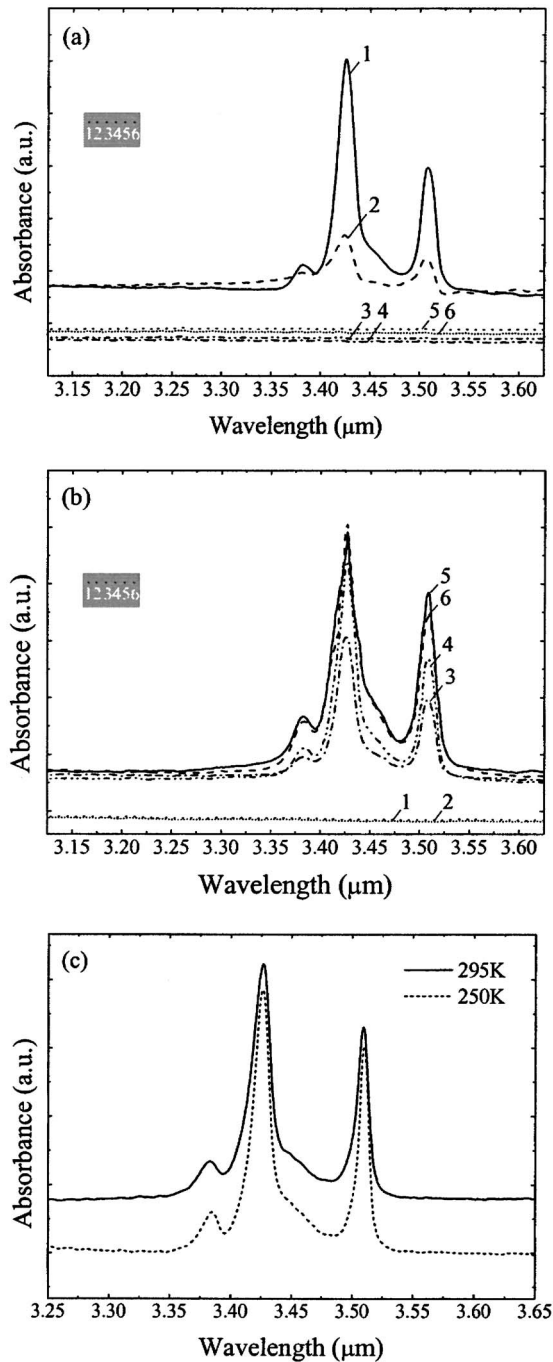


FIG. 4. Absorbance spectra. (a) 560 °C bonded structure. (b) 680 °C bonded structure. (c) 560 °C bonded structure measured at 295 and 250 K respectively.

areas in both samples annealed at high- and low-temperature as shown in Fig. 1. The reason is that with the increase of annealing temperatures, the decomposition and loss of interfacial materials were possibly enhanced.

As an example of application, FTIR absorbance spectra were used to examine interface quality of the bonded structures with InP- and GaAs-based epitaxial layers. An InP-based structure and a GaAs-based structure were directly bonded following the above method. The InP-based structure is a 35-period InP/InGaAsP distributed Bragg reflector

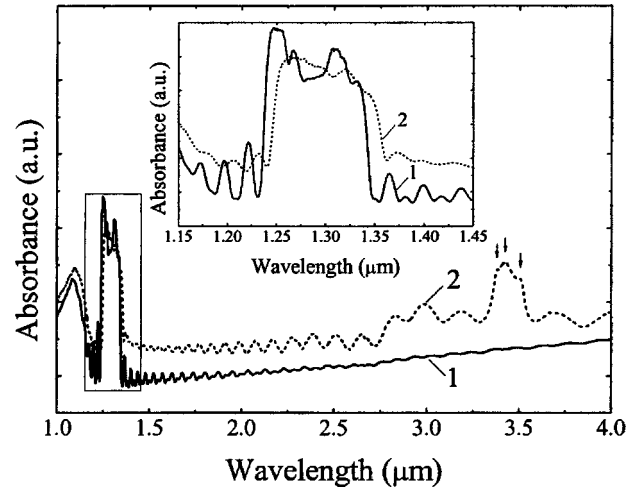


FIG. 5. Two-area absorbance spectra of the InP-based DBR followed by the PIN structure directly bonded to the GaAs-based DBR. The inset is the magnification image of the frame.

(DBR) followed by a P type-intrinsic-N type active layer. The GaAs-based structure is a 35-period AlGaAs/GaAs DBR. Before FTIR measurement, this wafer-bonded structure was processed with molten wax as well. Figure 5 shows the absorbance spectra at two different areas labeled 1 and 2. The spectrum 1 has no absorption peaks. However, three peaks around 3.426 μm appear in the absorbance spectrum 2. The redshift of the stop band (high-reflectivity region from 1.23 to 1.35 μm) of the spectrum 2 with respect of the spectrum 1 also indicates the increase of its cavity length. After chemically removing the InP substrate by aqueous-based $\text{HCl}+\text{H}_3\text{PO}_4$ (3:1) solutions, we found that the InP-based thin film in area 2 is bubbly and easily broken. Thus infrared-absorbance methods distinguish well-bonded areas which are candidates for device before fabrication.

C. Uniformity characterization of InP–GaAs bonded structures

To characterize interface quality of wafer-bonded InP–GaAs structures in direct view, absorbance intensity mappings (AIMs) were performed by FTIR measurements over different positions of bonded samples. By Eq. (4), if the wavelength for AIMs is selected at absorbance peaks (such as 3.426 μm), AIMs will characterize the thickness distribution of the interfacial gap that was filled with wax. Figure 6(a) shows the 3.426 μm AIM of the 560 °C bonded InP–GaAs structure. The dark color represents the higher absorption areas. The areas to the left of the dashed line have absorption peaks and thus gaps exist at the interface. Assuming maximum absorption occurs near $x=0$, we deduce that the dimension of these gaps gradually increases from the dashed line to the leftmost. This was verified by our FESEM observations. After cleavage along $y=4.5$ mm, the cross sections of this sample were observed by FESEM as shown in Figs. 6(b), 6(c), and 6(d) which are corresponding to areas 1, 2, and 3, respectively. The area 1 has a 20 nm-thick interfacial gap. The interface at area 3 is smooth and uninterrupted.

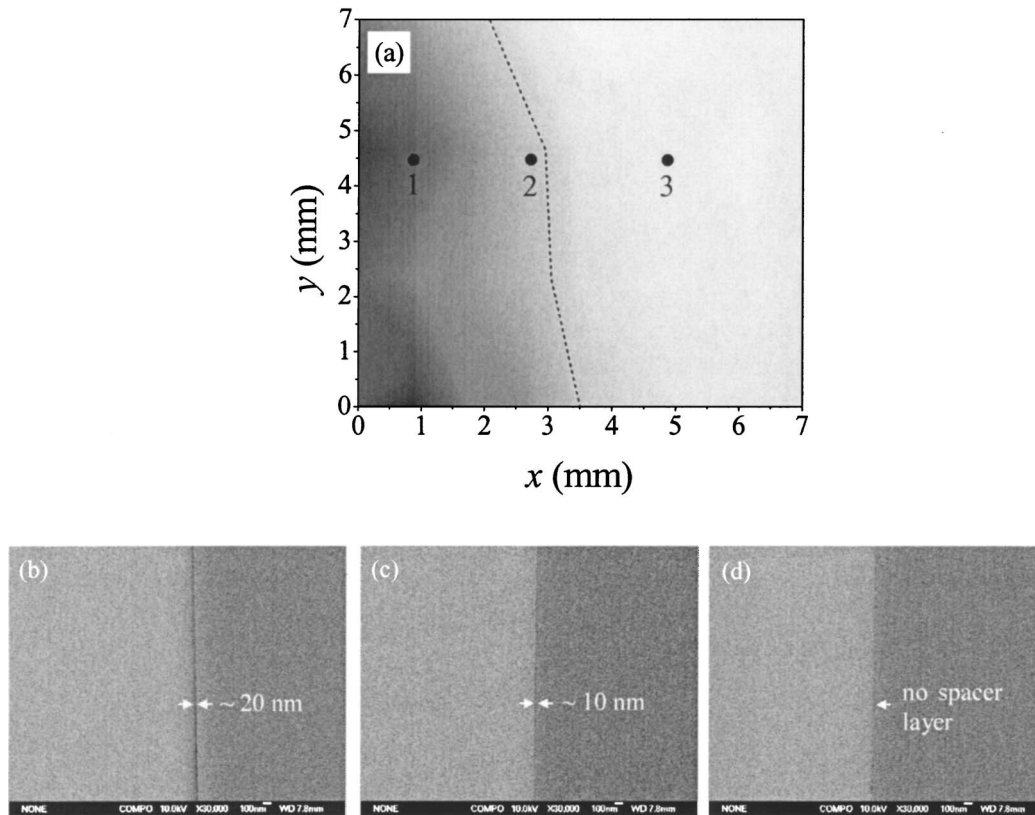


FIG. 6. (a) $3.426\ \mu\text{m}$ AIM of the InP-GaAs structure bonded at $560\ ^\circ\text{C}$ by the unimproved fixture in which three areas are labeled. Cross sections of (b) area 1, (c) area 2, and (d) area 3.

Thus the AIM in Fig. 6(a) is consistent with FESEM observations. Although the gap in area 2 is only 10 nm thick, the characteristic absorption of the wax in the gaps at the interface still makes it visible in the infrared spectra. This indicates that the wax-soaking technique is highly sensitive and nanoscale dimension of interface gaps could be detected.

From the observations of FESEM and AIM image shown in Fig. 6, it is reasonable to conclude that the nonuniformly bonded interface of the InP-GaAs structures could be caused by the nonuniformity of bonding pressure applied in the annealing step. However, it is experimentally difficult to detect pressure distribution during annealing process. To improve the bonding quality, we made a new bonding fixture which is focused on the improvement of pressure uniformity. By using this fixture, an InP-GaAs structure was directly bonded at $620\ ^\circ\text{C}$ and no absorption peaks around $3.426\ \mu\text{m}$ were observed as shown in Fig. 7. Standard deviation of absorbance-intensity data for the mapping in Fig. 7 is 0.048, while the standard deviation of data in Fig. 6(a) is 0.73. The improvement of pressure uniformity not only eliminates interfacial gaps but also extensively increases the interface uniformity of wafer-bonded InP-GaAs structures.

IV. CONCLUSIONS

In summary, we have directly bonded InP-GaAs structures under different temperatures. FESEM observations cannot inspect the interfaces of entire bonded samples because

its inspection size is limited to microregions. With the aid of wax soaking into poorly bonded interfaces, interfacial gaps have been detected by infrared-absorbance spectra. Nanoscale dimension of interface gaps can be detected using this method. AIMS at absorption peaks of wax were used to image poorly bonded areas. Thus the interface quality of the whole wafer-bonded sample can be seen clearly. Nonuniform pressure applied over the sample during annealing step accounts for poorly bonded interfaces. By improving the uni-

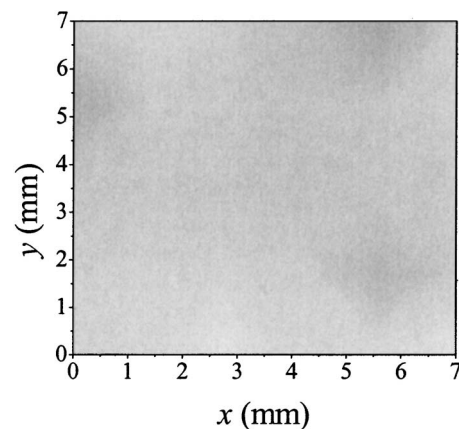


FIG. 7. $3.426\ \mu\text{m}$ AIM of the InP-GaAs structure bonded at $620\ ^\circ\text{C}$ by the improved fixture.

formity of pressure, uniformly bonded InP–GaAs structures that do not have interfacial gaps were obtained.

ACKNOWLEDGMENTS

This work was supported by the National Key Basic Research and Development Program of China under Grant No. 2003CB314903 and the Special Funding of Shanghai Nano-Promotion Center under Grant No. 0352NM092.

¹M. Shimbo, K. Furukawa, K. Fukuda, and K. Tanzawa, *J. Appl. Phys.* **60**, 2987 (1986).

²J. B. Lasky, *Appl. Phys. Lett.* **48**, 78 (1986).

³Z. L. Liao and D. E. Mull, *Appl. Phys. Lett.* **56**, 737 (1990).

⁴A. Black, A. R. Hawkins, N. M. Margalit, D. I. Babic, A. L. Holmes, Y. L. Chang, P. Abraham, J. E. Bowers, and E. L. Hu, *IEEE J. Sel. Top. Quantum Electron.* **3**, 943 (1997).

⁵L. Sagalowicz, A. Rudra, E. Kapon, M. Hammar, F. Salomonsson, A. Black, P.-H. Jouneau, and T. Wipijewski, *J. Appl. Phys.* **87**, 4135 (2000).

⁶F. Shi, K.-L. Chang, J. Epplé, C.-F. Xu, K. Y. Cheng, and K. C. Hsieh, *J. Appl. Phys.* **92**, 7544 (2002).

⁷Y. H. Lo, R. Bhat, D. M. Hwang, C. Chua, and C.-H. Lin, *Appl. Phys. Lett.* **62**, 1038 (1993).

⁸Y. L. Okuno, J. Geske, K.-G. Gan, Y.-J. Chiu, S. P. DenBaars, and J. E. Bowers, *Appl. Phys. Lett.* **82**, 2377 (2003).

⁹B. F. Levine, C. J. Pinzone, S. Hui, C. A. King, R. E. Leibenguth, D. R. Zolnowski, D. V. Lang, H. W. Krautter, and M. Geva, *Appl. Phys. Lett.* **75**, 2141 (1999).

¹⁰N. Y. Jin-Phillipp, B. Liu, J. E. Bowers, E. L. Hu, M. Kelsch, J. Thomas, and M. Ruhle, *Appl. Phys. Lett.* **80**, 1346 (2002).

¹¹J. Geske, Y. L. Okuno, J. E. Bowers, and V. Jayaraman, *Appl. Phys. Lett.* **79**, 1760 (2001).

¹²T. Akatsu, A. Plossl, R. Scholz, H. Stenzel, and U. Gosele, *J. Appl. Phys.* **90**, 3856 (2001).

¹³N. Y. Jin-Phillipp, W. Sigle, A. Black, D. Babic, J. E. Bowers, E. L. Hu, and M. Ruhle, *J. Appl. Phys.* **89**, 1017 (2001).

¹⁴H. Wada, Y. Ogawa, and T. Kamijoh, *Appl. Phys. Lett.* **62**, 738 (1993).

¹⁵R. J. Ram, J. J. Dudley, J. E. Bowers, L. Yang, K. Carey, S. J. Rosner, and K. Nauka, *J. Appl. Phys.* **78**, 4227 (1995).

¹⁶Y. Ohiso and C. Amano, *J. Appl. Phys.* **87**, 2857 (2000).

¹⁷G. Patriarche, F. Jeannes, J.-L. Oudar, and F. Glas, *J. Appl. Phys.* **82**, 4892 (1997).

¹⁸H. Wada and T. Kamijoh, *IEEE J. Sel. Top. Quantum Electron.* **3**, 937 (1997).